Macromolecules

Volume 28, Number 13 June 19, 1995

Synthesis of Liquid Crystalline Phosphazenes Containing Chiral Mesogens

Harry R. Allcock* and Eric H. Klingenberg

Department of Chemistry, The Pennsylvania State University, University Park, Pennsylvania 16802

Received December 27, 1994; Revised Manuscript Received March 17, 1995®

ABSTRACT: Phosphazene cyclic trimers and high polymers containing biphenyl side groups with (*S*)-2-methyl-1-butoxy as a terminal unit were synthesized. The chiral biphenyl units [4,4′-$C_6H_4C_6H_4OCH_2$-$CH(CH_3)CH_2CH_3$] were linked to the skeletal phosphorus atoms of the small-molecule phosphazene cyclic trimers and high polymers through $-O(CH_2CH_2O)_m-$ spacer linkages, where $m = 2$ or 3. Of the cyclic trimers synthesized, with the formula $N_3P_3[O(CH_2CH_2O)_mC_6H_4C_6H_4OCH_2CH(CH_3)CH_2CH_3]_6$ where $m =$ 2 (**4**) or 3 (**5**), only **5** was liquid crystalline, as determined by differential scanning calorimetry (DSC). Single-substituent high-polymeric poly(organophosphazenes) were synthesized that contained the chiral biphenyl unit linked to the backbone through spacer units $m = 2$ (**6**) and 3 (**8**). Cosubstituent polymers were also synthesized which contained both the chiral biphenyl derivative linked to the backbone through varying spacer lengths and with nonmesogenic cosubstituents, $OCH_2CH_2OCH_2CH_2OCH_3$ and OCH_2CF_3. The liquid crystalline behavior of these polymers was studied with respect to spacer length and nonmesogenic cosubstituents. All the polymers synthesized showed enantiotropic liquid crystallinity. Morphologies and thermal behavior of these compounds were investigated with the use of DSC, X-ray diffraction, and optical hot stage microscopy.

Introduction

Considerable interest exists in the synthesis and physical properties of polymeric liquid crystalline materials.[1-4] Liquid crystalline polymers (LCP's) combine the properties of small-molecule liquid crystals with characteristics generally associated with polymers, such as strength and ease of fabrication. Small-molecule liquid crystalline (LC) molecules have the ability to form well-ordered mesophases. These mesophases can be diverse in structure and often respond to external electric and magnetic fields. Polymers are typically lightweight and durable, can be easily processed, and have a high degree of dimensional stability. The combination of these two sets of properties allows the development of technologically useful materials.[5-7] Specifically, liquid crystalline polymers are of interest in the development of molecular switching devices, optoelectronic displays, and optical data storage devices.[8-10]

Polyphosphazenes are a broad class of macromolecules based on the repeating unit $(NPR_2)_n$. The properties of these macromolecules vary over a broad range depending on the side group structure.[11-13] Polyphosphazenes are well suited for the assembly of useful LCP systems because the phosphorus–nitrogen backbone is very flexible, and this can serve to enhance mesophase stability, thus increasing the useful temperature range over which these materials can be used.[14-17] The polyphosphazene backbone is also optically transparent in the visible region, which is an important feature in the development of optical devices.[18-22] These properties, combined with the ease with which the macromolecular properties can be modified by choosing the appropriate cosubstituents, make polyphosphazenes of considerable interest for both fundamental and applied research.

Earlier studies indicated that specific polyphosphazenes, especially those which contained fluoroalkoxy or aryloxy side groups, were capable of unusual mesophase behavior.[23-27] The exact nature of these mesophases is still not fully understood. However, single-substituent LC polyphosphazenes have been synthesized which contain rigid aromatic structures linked to the polymer through flexible alkoxy or alkyl groups.[28-37] The LC properties of these polymers are largely dependent on the nature of the mesogenic side group used and the length of the spacer between the mesogen and the polymer backbone. Three reports exist of LC polyphosphazenes that contain both mesogenic and

® Abstract published in *Advance ACS Abstracts,* May 15, 1995.

0024-9297/95/2228-4351$09.00/0

Scheme 1

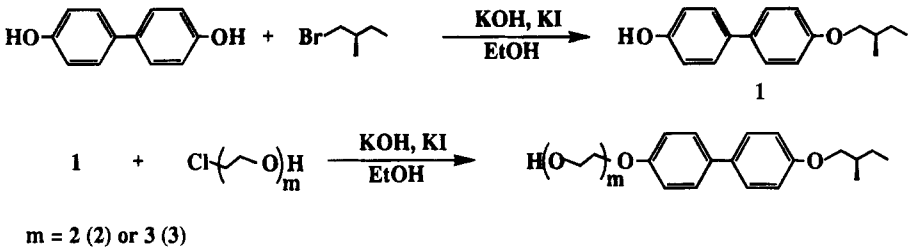

m = 2 (2) or 3 (3)

nonmesogenic cosubstituents. In all cases the trifluoroethoxy side unit was employed as the nonmesogenic side groups.[34-36]

Most of the LC polyphosphazenes examined to date exhibit LC mesophases that are of the smectic type. It has been demonstrated that compounds with smectic mesophases, particularly the smectic C mesophase, can be helielectric and ferroelectric, provided the mesogens have a large dipole moment across the short axis of the molecule. The proper alignment of the molecular dipoles is commonly accomplished by incorporation of chiral centers in the mesogenic molecules. Since Meyer first reported the ability of LC materials to be ferroelectric,[38] many reports have appeared concerned with the synthesis and properties of these types of LC materials.[39,40] Shibaev and co-workers were the first to report the synthesis of side-chain LCP's which were ferroelectric.[41] However, chiral LC materials which do not form a smectic C mesophase also show interesting electrooptical properties.[42-44] Liquid crystalline compounds which generate both nematic and nontilted smectic phases can be useful as either passive or active components. Such uses include polarizers, holographic elements, thermographical tools, optical switches, and image elaborators.[45]

Polyphosphazenes containing chiral azoxybenzene derivatives as mesogenic side groups were studied earlier in our program.[28] These polymers had very broad mesophase temperature ranges, exhibited tilted smectic mesophases, and had spontaneous polarization values similar to those observed for small-molecule LC compounds. Until now this has been the only report of polyphosphazenes which contained chiral mesogens.

In this paper we report the synthesis of a new series of LC polyphosphazenes with chiral biphenyl derivatives as the mesogenic side group substituents. The effects of spacer length on the LC behavior of the polymers was investigated. Cosubstituent polymers were also synthesized which contained either mesogenic and nonmesogenic cosubstituents or the same mesogenic group connected to the polymer chain through spacer units of varying lengths. The examination of such cosubstituent polymers allows a better understanding to be obtained of the effects that macromolecular cosubstituents have on the LC properties of phosphazene polymer systems.

Results and Discussion

Synthesis and Characterization. The commercially available chiral unit (*S*)-1-bromo-2-methylbutane was allowed to react with 4,4'-dihydroxybiphenyl to yield the monoetherification product (Scheme 1). Compound **1** was then coupled to the ethyleneoxy spacer linkages by a similar reaction to yield compounds **2** and **3** (Scheme 1). The chiral carbon was not directly involved in either reaction and, as a consequence, it remained unaffected. All compounds were white crystalline materials that were characterized by mass spectrometry, ^{1}H nuclear magnetic resonance (NMR) spectroscopy, and ^{13}C NMR spectroscopy.

The phosphazene cyclic trimers were synthesized by the procedure illustrated in Scheme 2. Cyclic trimers **4** (m = 2) and **5** (m = 3) are white crystalline solids that are soluble in most common organic solvents. The cyclic trimers were characterized by ^{1}H, ^{13}C, and ^{31}P NMR spectroscopy.

Poly(dichlorophosphazene) was prepared by the thermal ring-opening polymerization of hexachlorocyclotriphosphazene.[13] The desired poly(organophosphazenes) were then synthesized by the nucleophilic displacement of the chlorine atoms as illustrated in Scheme 2. Structural characterization of the polymers was performed by ^{1}H, ^{13}C, and ^{31}P NMR spectroscopy and by elemental analysis (Table 1 and Chart 1). The complete displacement of the chlorine atoms was confirmed by the existence of a singlet resonance in the ^{31}P NMR spectrum for each polymer and by elemental analysis where applicable.

All the polymers synthesized were off-white powdery materials. The single-substituent polymers were soluble in hot THF solutions, while the solubility of the cosubstituent polymers depended mainly on the nonmesogenic macromolecular cosubstituent. In general, all the cosubstituent polymers synthesized were more soluble in organic solvents than were the single-substituent polymers. This difference in solubility can be attributed to the ability of the cosubstituents to disrupt side group crystallinity.

Liquid Crystalline Behavior. Compounds **1**–**3** and the phosphazene cyclic trimer **4** were not liquid crystalline as determined by differential scanning calorimetry (DSC) and optical hot stage microscopy experiments. However, cyclic trimer **5** does exhibit monotropic LC behavior between 115 and 109 °C as determined by DSC experiments and optical hot stage examination. The schlieren texture observed in optical hot stage experiments with $-1/2$ and $+1/2$ singularities suggests that the mesophase is nematic in structure.[3]

All the high polymers synthesized were enantiotropic LC materials. Attachment of the biphenyl groups to the polymer chain hinders the melting process and allows the appearance of a mesophase. This difference between the thermal behavior of the polymers and the small-molecule compounds is known as the "polymeric effect".[1-4] The thermal transitions measured for the polymers by DSC were all relatively broad in range, ca. 10–15 °C. The width of the thermal transitions is most likely due to the molecular weight polydispersity of the polymer samples. All the polymers synthesized had polydispersities of ca. 1.9–3.5. In such a disperse system the lower molecular weight species are more likely to undergo the thermal transitions at lower temperatures than are the higher molecular weight components. The differences in these transition temperatures cause the transitions to occur over a wider

Scheme 2

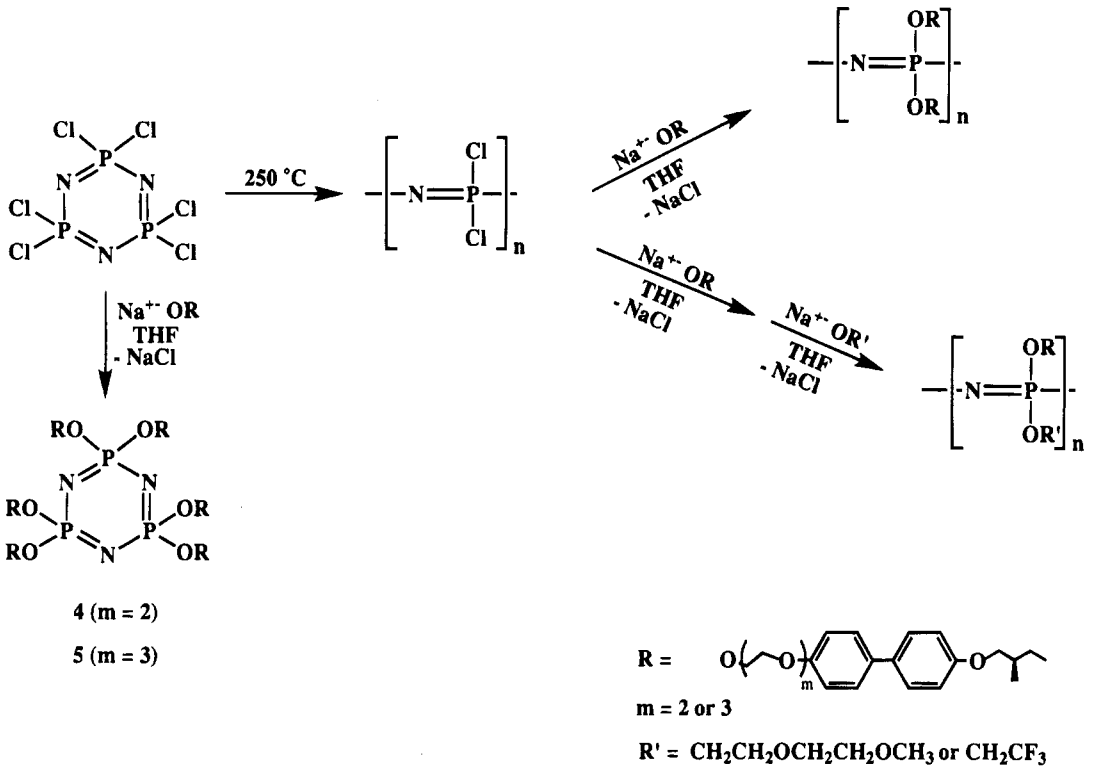

range of temperatures than would be the case for polymers having a low polydispersity.

There were no glass transitions detected for these polymer systems. This is most likely due to the mesogenic side chains crystallizing before the polymers reach their glass transition temperature. This was not unexpected since polyphosphazenes generally have very low glass transition temperatures.[13]

Polymers with the Biphenyl Unit Linked to the Backbone through Diethyleneoxy Spacer Groups. Polymers **6**–**8**, which contain the biphenyl unit linked to the polymer backbone through diethyleneoxy spacer linkages, all showed similar LC mesophases. These polymers displayed cholesteric (Ch) and smectic A (Sa) mesophases as identified by optical hot stage microscopy and X-ray diffraction. Polymer **6** was liquid crystalline between the temperatures of 125 and 226 °C (Tables 2 and 3 and Figure 1). The Sa to Ch transition occurred at 174 °C on heating. The X-ray diffraction pattern of **6**, which was quenched at 180 °C, showed only a diffuse ring. This is consistent with nematic type ordering. However, because the side groups contain a chiral center, this type of mesophase is then designated as either a twisted nematic or a cholesteric phase: for the purposes of this paper it will be referred to as the cholesteric phase (Ch). The optical micrographs taken during the cooling of **6** from the isotropic phase appeared as long thin batonnets or "cracks". This texture is consistent with those of previously identified polymeric Ch mesophases.[4] With further cooling these batonnets appear to coalesce to form a focal conical fan texture. X-ray diffraction experiments on polymer **6** quenched at 135 °C revealed that the fan texture is a layered structure which corresponds to the Sa type ordering. Side group length was calculated using Quanta 3.0[48] and was found to be 22.04 Å. The layer spacing determined from X-ray diffraction experiments was calculated to be approximately 42.5 Å (Table 4). This suggests that the layered planes consist of two sets of side group molecules which overlap slightly, and this is consistent with the structure of the smectic mesophases of previously studied LC polyphosphazenes (Figure 2).[28–31]

Polymers **7** and **8** show the same mesophases as **6**. This is in contrast to previously studied phosphazene systems in which the LC mesophases for the copolymers were less ordered than the mesophases observed for the homopolymers.[34,35,46] However, the previously studied systems contained larger amounts of the nonmesogenic cosubstituents than those copolymers studied here. The relatively low amounts of nonmesogenic cosubstituents contained in the polymer systems presented here, less than 27% of the total substitution, may be the reason for polymers **6** and **7** exhibiting the same mesophases. X-ray diffraction experiments on **7** indicate that the layer-like order is lost as the temperature is raised, similar to **6** (Table 4). This behavior was also observed with **8**. The isotropization temperatures for **7** and **8** are lower than those observed for **6**. This is probably due to the nonmesogenic side groups breaking up the crystalline packing of the biphenyl substituents. The Sa to Ch transition for **7** occurs at 135 °C and is consistent with the idea that the nonmesogenic side groups interfere with the crystalline packing of the mesogenic groups. However, **8** shows the same transition at 195 °C, approximately 20 °C higher than the same transition for **6**, which occurs at 174 °C. The difference in the Sa–Ch transition temperatures for **6** and **8** is not easily explained. The higher Sa–Ch transition temperature of **8** (195 °C) could be a result of an ordering of the trifluoroethoxy substituents. It is known that poly[bis(trifluoroethoxy)phosphazene] is capable of unusual mesophase formation.[23–27] Also, it has been observed in polymer-dispersed LC systems that the mixing of small-molecule LC compounds with polymers is considerably less when the polymer is fluorinated.[47] Therefore, the differences in the structural characteristics of the trifluoroethoxy group and the

Table 1. Characterization Data for the Phosphazene Cyclic Trimers and High Polymers

compd	^{31}P NMR (ppm)	^{13}C NMR (ppm)	^{1}H NMR (ppm)	elemental anal. % calc (% found)	mol. wt (GPC) M_w (M_w/M_n)
4	18.5 (s)	11, 17, 27, 35, 73, 115, 116, 129, 129.5, 133, 134, 154, 158	0.98 (t, CH_3), 1.04 (d, CH_3), 1.30 (m, CH_2), 1.60 (m, CH_2), 1.89 (m, CH), 3.82–4.20 (m, OCH_2), 7.45–6.97 (ArH)		
5	18.0 (s)	11, 17, 27, 35, 62, 67.5, 69.5, 72, 72.5, 115, 127, 133, 134, 150	0.96 (t, CH_3), 1.05 (d, CH_3), 1.27 (m, CH_2), 1.60 (m, CH_2), 1.86 (m, CH), 3.74–4.16 (m, OCH_2), 7.45–6.97 (ArH)		
6	−7.2 (s)	11, 17, 27, 35, 62, 67, 69, 70, 70.5, 71, 72, 72.5, 115, 127, 132, 133, 157, 158	0.65–0.98 (CH_3), 1.02–1.15 (CH_2), 1.20–1.32 (CH_2), 1.51–1.70 (CH), 3.2–4.1 (CH_2), 6.3–7.2 (ArH)	C, 69.0 (68.4) N, 2.00 (1.84) H, 7.17 (7.20) Cl, <1 (0.03)	$[\eta]$ = 1.24 dL/g[b]
7	−6.8 (s)	11.0, 17.2, 25.4, 34.9, 64.9, 65.1, 67.5, 70.0, 71.8, 72.3, 114.2, 126.4, 132.5, 133.0, 157.7, 158.1	0.70–1.10 (CH_3), 1.20–1.40 (CH_2), 1.45–1.61 (CH_2), 1.70–1.80 (CH), 3.00–4.70 (OCH_2), 6.20–7.64 (ArH)	C, 65.9 (65.1) N, 1.90 (2.16) H, 7.43 (7.77) Cl, <1 (0.04)	3.62×10^5 (2.55)
8	−7.3 (s)	12.1, 17.0, 26.4, 35.0, 65.1, 67.1, 69.5, 71.2, 73.2, 114.1, 128.0, 133.1, 157.5, 158.2	0.80–1.15 (CH_3), 1.21–1.43 (CH_2), 1.53–1.74 (CH_2), 1.76–1.98 (CH), 3.00–4.81 (OCH_2), 6.30–7.53 (ArH)	C, 67.1 (67.5) N, 2.42 (2.67) H, 7.13 (6.91) Cl, <1 (0.05)	8.04×10^5 (2.06)
9	−6.8 (s)	11.6, 16.5, 26.1, 34.8, 62.1, 68.2, 70.2, 72.6, 73.2, 114.7, 127.8, 133.9, 156.5, 158.2	0.80–1.12 (CH_3), 1.22–1.31 (CH_2), 1.32–1.39 (CH_2), 1.81–1.90 (CH), 3.01–4.95 (OCH_2), 6.45–7.62 (ArH)	C, 67.4 (68.1) N, 1.73 (1.84) H, 7.60 (7.47) Cl, <1 (0.03)	$[\eta]$ = 1.63 dL/g[b]
10	−6.3 (s)	11.7, 16.4, 26.2, 35.0, 62.1, 68.2, 70.2, 73.1, 73.4, 74.0, 114.6, 127.9, 133.1, 134.0, 156.7, 158.4	0.85–1.12 (CH_3), 1.14–1.35 (CH_2), 1.46–1.68 (CH_2), 1.72–1.91 (CH), 3.18–4.56 (OCH_2), 6.45–7.49 (ArH)	C, 64.2 (62.6) H, 7.62 (7.57) N, 2.12 (2.10) Cl, <1 (0.10)	4.55×10^5 (2.66)
11	−6.9 (s)	11.7, 16.5, 26.1, 34.7, 62.1, 64.2, 68.2, 70.2, 73.1, 73.5, 114.6, 127.9, 133.1, 134.0, 156.5, 158.2	0.85–1.15 (CH_3), 1.17–1.28 (CH_2), 1.47–1.69 (CH_2), 1.75–1.96 (CH), 3.42–4.45 (OCH_2), 6.54–7.53 (ArH)	C, 65.3 (65.6) H, 6.95 (7.71) N, 2.13 (1.88) Cl, <1 (0.01)	5.37×10^5 (2.03)
12	−7.2[a]	11.0, 16.5, 26.3, 35.0, 65.1, 66.0, 69.7, 70.5, 72.7, 114.5, 127.0, 131.9, 132.5, 157.5, 158.2	0.71–1.08 (CH_3), 1.11–1.24 (CH_2), 1.42–1.63 (CH_2), 1.65–1.89 (CH), 3.37–4.55 (OCH_2), 6.30–7.41 (ArH)	C, 68.5 (67.1) N, 1.97 (2.05) H, 7.44 (7.28) Cl, <1 (0.24)	2.73×10^5 (2.17)
13	−6.1[a]	11.5, 14.6, 26.4, 34.8, 65.1, 65.9, 67.0, 69.1, 70.4, 72.5, 114.5, 127.2, 132.5, 157.5, 158.2	0.75–1.05 (CH_3), 1.06–1.20 (CH_2), 1.32–1.65 (CH_2), 1.71–1.95 (CH), 2.81–4.45 (OCH_2), 6.05–7.43 (ArH)	C, 68.1 (68.5) N, 1.85 (1.93) H, 7.49 (7.17) Cl, <1 (0.48)	2.06×10^5 (1.98)
14	−4.9[a]	11.5, 14.6, 26.4, 34.8, 65.1, 65.9, 67.0, 69.1, 70.4, 72.5, 114.5, 127.2, 132.5, 157.5, 158.2	0.75–1.15 (CH_3), 1.18–1.43 (CH_2), 1.47–1.71 (CH_2), 1.75–1.98 (CH), 3.05–4.47 (OCH_2), 6.43–7.44 (ArH)		7.77×10^5 (3.43)

[a] Peaks were broad. [b] Viscosities were measured in $CHCl_3$ at 35 °C using a Cannon-Ubbelohde viscometer.

chiral biphenyl unit with the attached spacer may result in the formation of microdomains. However, investigations using transmission electron microscopy and scanning electron microscopy have yet to provide additional evidence for domains. It is also possible these polymers possess some block type structure. This is not easy to determine by ^{31}P NMR experiments since the chemical shifts for phosphorus atoms that bear trifluoroethoxy and the chiral biphenyl units both occur at ca. −7 ppm. Precautions were taken during the synthesis of these polymers to reduce the formation of block structure by the very slow addition of the alkoxide salts to the polymer and by the use of dilute reaction solutions. Thus, it is believed that the side group dispersion is essentially random. However, it is not clear if microdomain formation, the presence of blocks of trifluoroethoxy cosubstituents, or both result in the mesophase stabilization.

The textures of the LC phases for polymers **7** and **8** are identical to the textures observed for **6**. Following cooling from the isotropic melt, all the polymers initially have textures which appear as very long thin batonnets or "cracks" (Figure 3). These "cracks" then change quickly into the focal conical fan texture when cooled to the respective Ch to Sa transition temperatures.

Polymers Which Contain the Biphenyl Groups Linked to the Backbone through Triethyleneoxy Spacer Groups. The mesophase temperature ranges for the polymer series **9**–**11** are narrower than the ranges found for **6**–**8** (Tables 2 and 3). The mesophase range for polymer **9** is approximately 46 °C wide, while the mesophase temperature range for polymer **6** is approximately 101 °C. A reason for the reduction in mesophase width is that the longer spacer linkage further decouples the motions of the biphenyl units from the motions of the flexible polymer backbone. This decoupling allows the side groups to act more independently from the polymer backbone. If total decoupling were to occur, there would be no mesophase formation at all because the biphenyl side groups are not liquid crystalline by themselves. Therefore, further decoupling the motions of the side groups from the backbone narrows the mesophase temperature range. This is in contrast to previously studied hydrocarbon- and siloxane-based polymer systems where increasing the spacer lengths generally increases the mesophase temperature ranges.[1,49] Polymers **9**–**11** have smectic mesophase structures, while polymers **6**–**8** have both smectic and cholesteric structures. The formation of higher ordered liquid crystalline states with further decoupling seems

Chart 1. Polymer Structure

$$-[NP(OR)_x(OR')_y(OR'')_z]_n-$$

R =

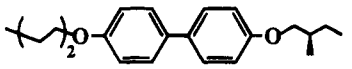

R' =

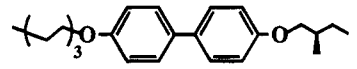

R'' = $CH_2CH_2OCH_2CH_2OCH_3$ (MEE) or CH_2CF_3 (TFE)

Polymer	x	y	z	R''
6	2	0	0	—
7	1.47	0	0.53	MEE
8	1.56	0	0.44	TFE
9	0	2	0	—
10	0	1.51	0.49	MEE
11	0	1.62	0.38	TFE
12	1.62	0.38	0	—
13	0.95	1.05	0	—
14	0.41	1.59	0	—

Table 2. Thermal Data for Phosphazene Polymers[a]

	thermal transitions[b]			mesophase	mesophase
compd	T_{K-LC}	T_{LC-LC}	T_{LC-I}	width (°C)[c]	structure
6	125 (116)	174 (148)	226 (200)	101	smectic A and cholesteric
7	121 (109)	135 (132)	198 (163)	77	smectic A and cholesteric
8	122 (115)	195 (179)	214 (193)	92	smectic A and cholesteric
9	101 (98)	113 (107)	147 (141)	46	smectic C* and smectic A
10	101 (82)		145 (112)	44	smectic A
11	115 (105)		169 (160)	54	smectic A
12	105 (100)	142 (132)	226 (194)	121	smectic A and cholesteric
13	112 (110)	156 (141)	251 (244)	139	smectic A and cholesteric
14	94 (93)		172 (150)	78	smectic

[a] Thermal transitions were made using a Perkin-Elmer DSC7 instrument with heating and cooling rates of 10 °C/min. [b] Thermal transitions in parentheses are taken from the cooling cycles on the DSC. [c] Mesophase width is calculated from the heating scans.

unlikely given that the side groups themselves are not liquid crystalline. A possible explanation for this behavior is that the shorter spacer linkages do not allow the rotational degrees of freedom necessary for the side groups to "melt" at the higher temperatures. Therefore, polymers **6**–**8** are capable of forming lower ordered LC states at higher temperatures.

The mesophase temperature range for **10** is narrower than that for **9**. This is probably because the (methoxyethoxy)ethoxy cosubstituent units break up the crystallinity of the biphenyl units. In contrast, polymer **11** has a mesophase range which is wider than that of **9**. This may be related to microdomain formation or blocky segments within the polymer as discussed above with respect to the Sa mesophase stabilization of polymer **8**.

Table 3. Enthalpy and Specific Optical Rotation Data for the Polymers[a]

polymer	ΔH_{K-LC}[b]	ΔH_{LC-LC}	ΔH_{LC-I}	$[\alpha]^{24}$ [c] (deg)
6	2.03 (1.74)	0.17 (0.14)	2.11 (1.94)	+7.48
7	0.99 (0.91)	0.10 (0.08)	0.43 (0.17)	+3.67
8	1.06 (0.80)	0.06 (0.40)	1.06 (0.80)	+2.79
9	2.34 (2.17)	0.75 (0.58)	2.15 (1.91)	+6.11
10	1.73 (1.20)		1.34 (1.27)	+3.72
11	1.64 (1.34)		0.88 (0.56)	+5.64
12	1.59 (1.24)	0.13 (0.12)	1.11 (0.97)	+3.81
13	1.78 (1.48)	0.16 (0.13)	0.54 (0.39)	+2.81
14	1.52 (1.25)		0.49 (0.27)	+4.44

[a] All enthalpies are reported in kcal/mol of repeat unit. [b] Enthalpies recorded on cooling are shown in parentheses. [c] Polarimetry experiments were performed in $CHCl_3$ with λ = 589 nm.

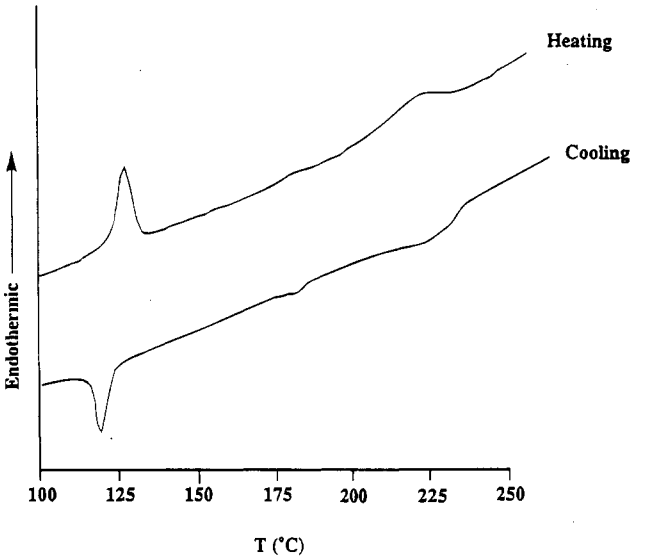

Figure 1. Typical DSC trace for the LC polymers. The DSC trace shown is for polymer **6**. Enantiotropic mesophases occur on both heating from the crystalline solid and cooling of the isotropic liquid. Monotropic mesophases occur only on cooling from the isotropic liquid. All polymers in this study were enantiotropic LC's.

Table 4. X-ray Diffraction Data for Phosphazene Polymers

		d spacings (Å)				
compd	temp (°C)[a]	d_1	d_2	d_3	d_4	layer spacing (Å)
6	180	*b*				
	135		21.3	14.2	10.5	42.4
7	150	*b*				
	130	42.8	21.4	14.3		42.8
8	200	*b*				
	150		22.6	15.5	11.8	45.1
9	135		23.3	15.5	11.7	46.6
	108		22.3	14.9	11.2	44.7
10	125		23.2	15.4	11.5	46.2
11	130		23.4	15.4	11.7	46.6
12	210	*b*				
	135		23.3	15.3	11.7	46.4
	110	42.2	21.2	14.4	8.68[c]	42.9
13	180	*b*				
	140	42.6	21.3	14.3	8.56[c]	42.7
14	150		22.3	14.9	11.6	44.7

[a] Films were quenched at these temperatures by quickly placing the slide on a liquid N_2 cooled metal plate. [b] Only a broad amorphous ring was observed in the diffraction pattern. [c] Numbers correspond to d_5.

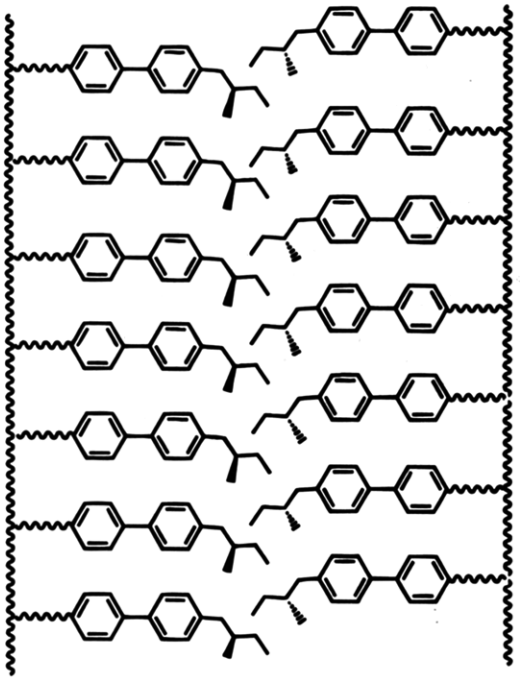

Figure 2. Representation of the layered planes in the smectic mesophases.

A.

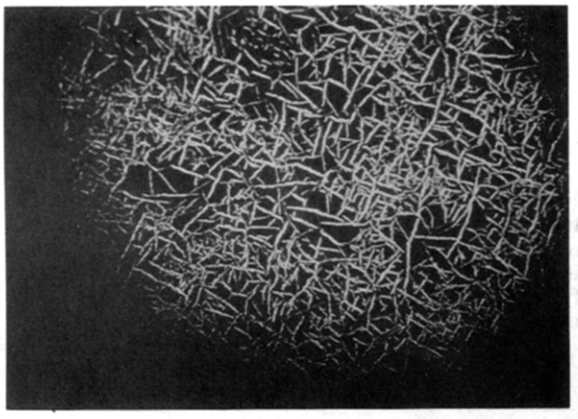

B.

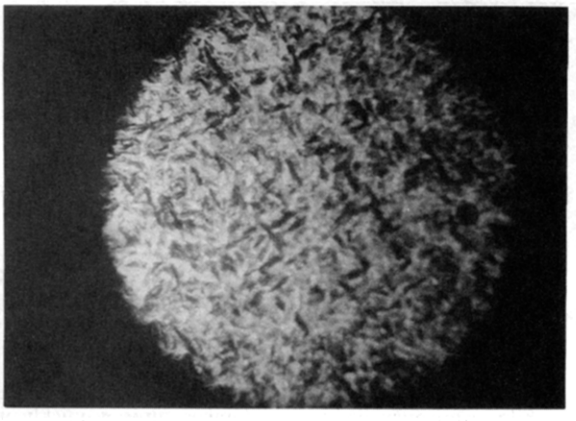

Figure 3. Optical micrographs of the different mesophase textures for polymer **8**: (A) Ch (×75 at 185 °C) (the application of shear to this phase produces a planar texture); (B) Sa (×60 at 150 °C).

Polymer **9** has two different mesophase morphologies, Sa and smectic C* (Sc*). The Sa mesophase exists between 113 and 147 °C, while the Sc* mesophase exists between 101 and 113 °C. The mesophase morphologies were determined by optical hot stage microscopy and X-ray diffraction. The calculated side group length was 26.61 Å and the layer spacing calculated from the X-ray diffraction experiments was 47.2 Å for the Sa mesophase and 44.7 Å for the Sc* mesophase. This corresponds to layered structures in which there is a slight overlap of the alkyl tails. In the Sc* mesophase, the smaller layer spacing is believed to result from additional factors beyond the overlap of the alkyl tail groups. Since branching exists within the tail groups, it is unlikely that layered mesophase structures could be formed in which a large degree of overlap exists between the side groups. It is more probable that the side groups are tilted with respect to the layered planes. The tilt angle associated with this mesophase is not very large because the range in which the Sc* mesophase occurs is narrow. Therefore, it appears that the molecules are just beginning to tilt when the polymer crystallizes. The Sc* mesophase appearance was schlieren (Figure 4A), and the Sa mesophase was focal conical fan textured. Polymers **10** and **11** showed only Sa mesophase textures as determined by optical hot stage microscopy and X-ray diffraction. The layer spacings calculated from X-ray diffraction experiments for polymers **10** and **11** were 46.2 and 46.6 Å, respectively. Polymer **10** has a focal conical fan mesophase texture consistent with the Sa mesophase characterization (Figure 4B). The mesophase texture for **11** is much finer than that observed for **10**. The focal conical fan texture for polymer **10** is generally perpendicular to the field of vision while those for polymer **11** seem to be parallel to the field of vision. The parallel alignment of the fan texture results in a mesophase structure which appears as small circles (Figure 4C). Further observations of this texture using higher magnifications revealed the presence of a maltese cross through the circles, consistent with the Sa characterization.

Polymers Which Contain the Biphenyl Units Linked to the Backbone through Tri- and Diethyleneoxy Spacer Groups. The cosubstituent polymers with mixed spacer lengths, **12**–**14**, have very broad mesophase ranges (Tables 2 and 3). Polymers **12** and **13** contain 75 and 50% of the chiral biphenyl linked to the backbone through diethyleneoxy spacer linkages, respectively. The remainder of the macromolecular cosubstituents are the chiral biphenyl units linked to the polymer through triethyleneoxy spacer linkages. These species have the widest mesophase temperature ranges of all the polymers in this study, with mesophase widths of 121 (**12**) and 139 °C (**13**). The mesophase range for **14**, which contains 75% of the chiral biphenyl linked to the backbone through the triethyleneoxy spacer unit, is 78 °C. The increase in mesophase width for these copolymers is most likely a dilution effect similar to that seen when small-molecule liquid crystalline molecules that are closely related in structure are mixed together. Current LC technologies use such mixtures to broaden the useful temperature range over which the LC material can be used. This effect also occurs in other polymer systems and is a good indication that by mixing similar side group mesogens it is possible to further tune the polymer properties to obtain useful materials over a wide range of temperatures.

Three different mesophases were observed for polymer **12** by optical hot stage microscopy. The first mesophase appears as long streaks and is probably cholesteric in nature (Figure 5A). X-ray diffraction supports this assignment with only a broad diffuse ring

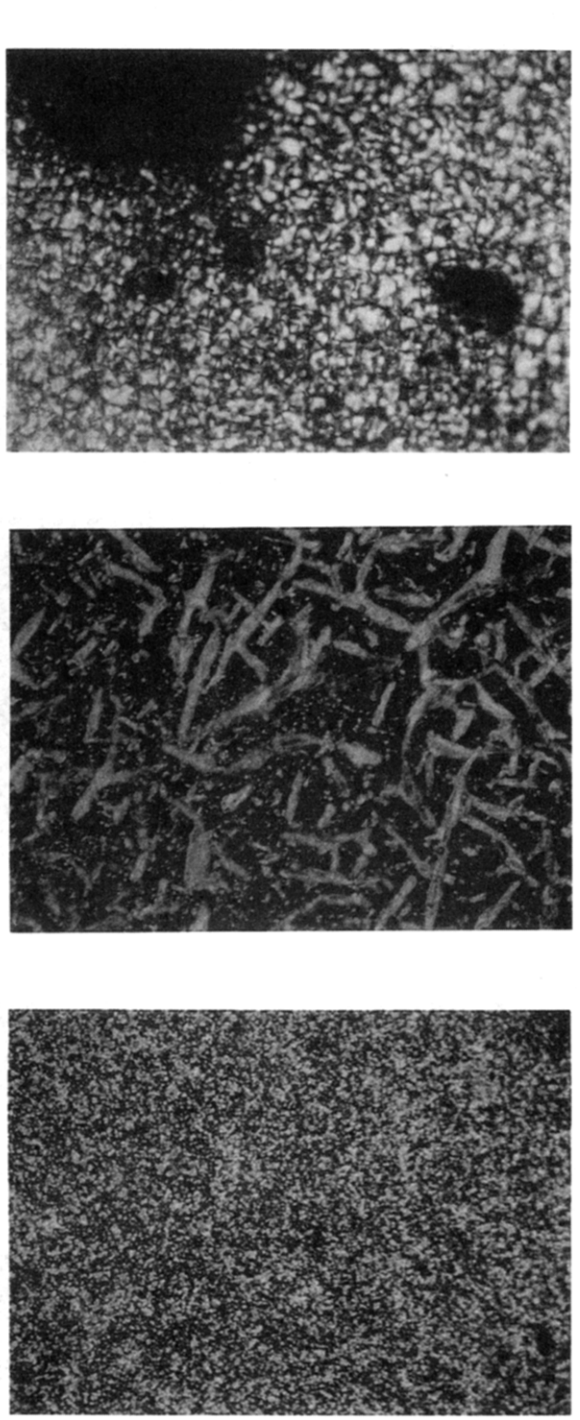

Figure 4. Optical micrographs of the mesophase textures for polymers **9**–**11** (×140): (A) Sc* for **9** (105 °C); (B) Sa for **10** (110 °C); (C) Sa for **11** (130 °C).

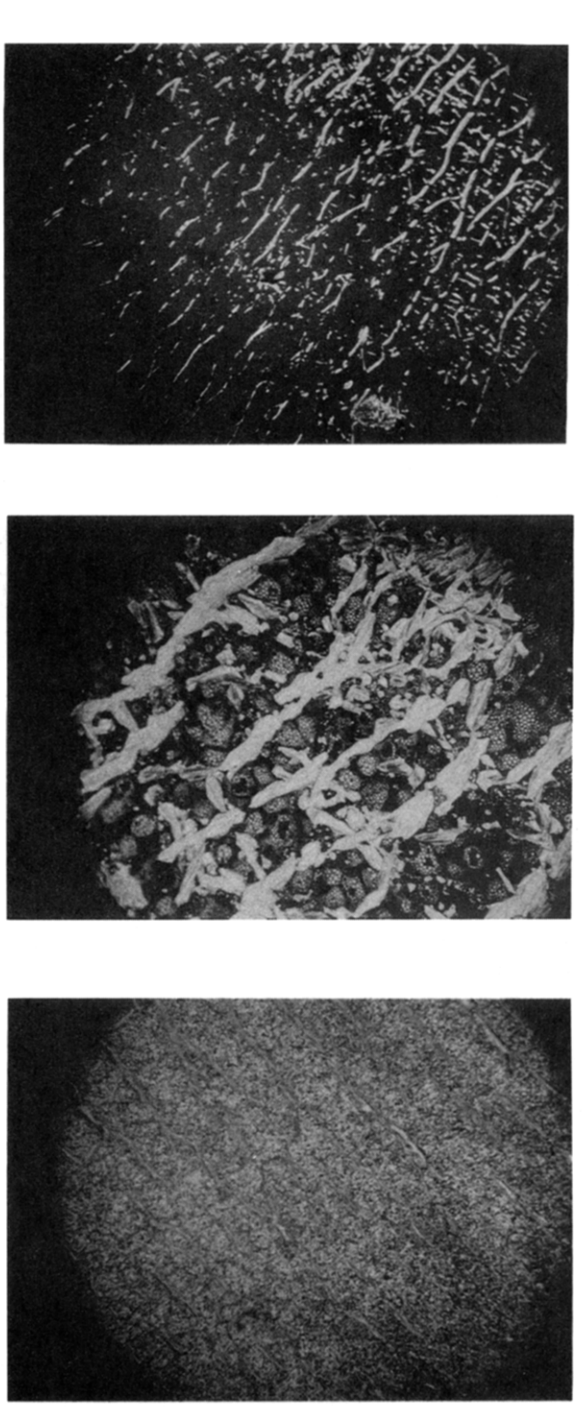

Figure 5. Optical micrographs of the mesophase textures for polymer **12** (×75): (A) Ch (180 °C); (B) Sa (135 °C); (C) Sc* (113 °C).

detected in the diffraction pattern, which corresponds to the amorphous-like character of the polymer in this state. With further cooling, these cholesteric streaks change into a focal conical fan type texture. Interestingly, the portions of the polymer film between where the cholestric streaks were in Figure 5A are oriented differently from the portions of the film which appeared as cholestric streaks in Figure 5A (Figure 5B). The fans between the cholesteric streaks had the focal conical fans oriented parallel to the line of sight, which appeared as small circles with a cross in the middle. The cholesteric streak portions of the polymer film had the focal conical fans oriented perpendicular to the line of sight and looked more like the typical fan texture. A third mesophase, which was schlieren textured, was observed on further cooling to ca. 115 °C (Figure 5C). This transition was not detected in the DSC, probably because of the very small change in energy associated with the change from a Sa to a Sc* texture. X-ray diffraction experiments indicated that the Sa mesophase has a layer spacing of approximately 46.2 Å while the Sc* mesophase has a spacing of 42.9 Å.

Polymer **13** generates two different mesophases: a Ch mesophase and a Sa mesophase. The Ch mesophase appears as very small dots during cooling from the isotropic state. These dots then change into a focal conical fan texture on cooling to ca. 140 °C (Figure 6). The layer spacing for the Sa mesophase is 42.7 Å as determined by X-ray diffraction experiments.

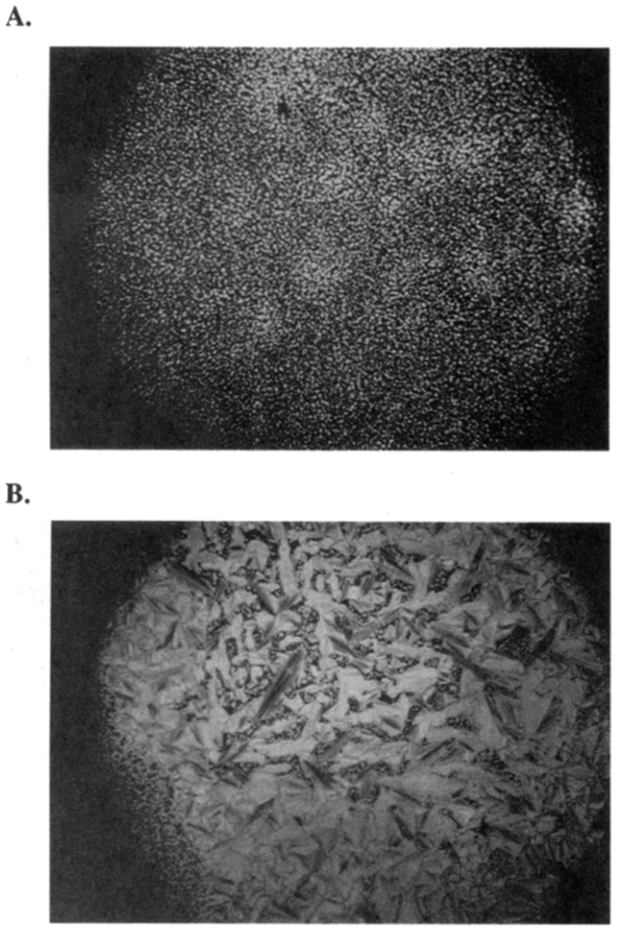

Figure 6. Optical micrographs of the mesophase textures for polymer **13** (×75): (A) Ch (200 °C); (B) Sa (130 °C).

The mesophase textures of **14** correspond to a Ch system and a higher ordered smectic mesophase. Batonnets are observed when the system is cooled from the isotropic state (see Figure 7). This texture existed for a temperature range of ca. 5 °C, at which time the batonnets appeared to "pinch off" into a very fine schlieren-like texture. The Ch mesophase was not detected in the DSC experiments because of the overlap with the isotropization endotherm. The smectic mesophase has a layer spacing of 44.7 Å. It was unclear if the mesophase is of the Sa type or of the Sc* type.

All the cosubstituent polymers with mixed spacer lengths showed no significant disordering from the mixing of mesogens since most of the polymers studied showed higher ordered smectic mesophases. These cosubstituent polymers also have increased solubility in organic solvents and very broad mesophase temperature ranges, which are useful attributes when considering device applications.

Conclusions

Only one of the small-molecule model cyclotriphosphazenes showed LC behavior. Compound **5** showed a monotropic LC mesophase which was nematic on cooling from the isotropic melt.

Polyphosphazenes containing chiral biphenyl units showed enantiotropic LC behavior. Single-substituent polymers bearing only biphenyl units were generally less soluble than were the mixed-substituent polymers. The liquid crystalline behavior of the polymers depended on the nature of the cosubstituents. The more highly ordered mesophases are obtained with the single-

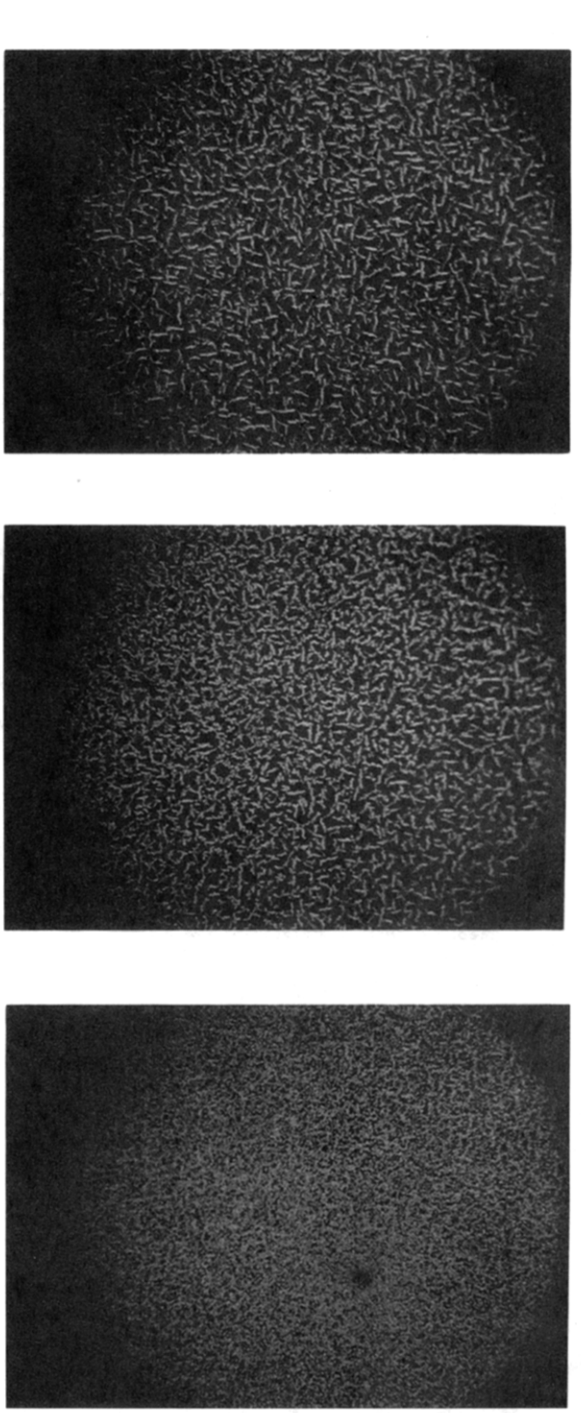

Figure 7. Optical micrographs of the mesophase textures for polymer **14** (×75): (A) Ch (147 °C); (B) Ch to smectic transition (142 °C); (C) smectic mesophase (120 °C).

substituent polymers and with mixed-substituent polymers that contained biphenyl units linked to the backbone with mixed spacer lengths. Polymers which contained only diethyleneoxy spacer groups had Sa and Ch mesophase structures. However, polymers with triethyleneoxy spacer groups generated only smectic mesophases and narrower mesophase temperature ranges. The narrowing of the mesophase temperature ranges with increasing spacer lengths is unexpected, since previous studies on non-phosphazene-based systems have shown increasing mesophase ranges and more highly ordered mesophase structures with increasing spacer lengths.[1,49]

Cosubstituent polymers with (methoxyethoxy)ethoxy cosubstituents had less ordered mesophases, or the more

highly ordered mesophase existed over a smaller temperature range than for the corresponding single-substituent polymers. Engel and co-workers have reported work on the effects of nonmesogenic cosubstituents on methacrylate systems.[49,50] They have found that with relatively small amounts of the nonmesogenic cosubstituents the mesophases can be stabilized, which is similar to the results in this study. Increasing nonmesogenic character destabilizes the mesophases and can result in lower mesophase temperature ranges and less ordered mesophases. However, the trifluoroethoxy cosubstituent polymers had wider Sa mesophases than those copolymers which contained (methoxyethoxy)ethoxy cosubstituents. The reason for this is still unclear.

The most interesting systems were those copolymers with mixed spacer lengths. These polymers were capable of forming higher ordered smectic mesophases and had very broad mesophase temperature ranges. These are generally the most important characteristics when choosing a polymer system for device applications. This is very similar to other polymer systems where variations in the spacer length within a polymer system can result in polymers with increased mesophase stability.[49,51] The electrooptical properties of these polymers are currently being investigated.

Experimental Section

Materials. All solvents were dried over sodium using benzophenone as an indicator or over calcium hydride and were freshly distilled before use. All reagents (Aldrich) were used as received. Silica gel (70−260 mesh, Aldrich) was used for column chromatography. Hexachlorocyclotriphosphazene provided by Ethyl Corp. was purified by recrystallization from heptane followed by vacuum sublimation at 40 °C (0.50 mmHg). Poly(dichlorophosphazene) was prepared by the thermal melt polymerization of $(NPCl_2)_3$ at 250 °C. An average of 35−50% conversion to the high polymer was obtained.

Instruments. ^{31}P (144.8 MHz), ^{1}H (360.0 MHz), and ^{13}C (90.0 MHz) NMR spectra were recorded with the use of a Bruker WM360 NMR spectrometer, which employed a broadband CPMAS pencil probe. Chemical shifts are relative to external 85% H_3PO_4 (^{31}P NMR) or tetramethylsilane (^{1}H and ^{13}C NMR). All heteronuclear NMR spectra were proton decoupled. Molecular weights were determined by using a Hewlett-Packard HP1090 gel permeation chromatograph equipped with an HP-1037A refractive index detector and a Polymer Laboratories PL Gel 10-μm column. The samples were eluted with a 0.1% by weight solution of tetra-*n*-butylammonium bromide in THF. The GPC column was calibrated with polystyrene standards (Waters). Thermal analyses were carried out using a Perkin-Elmer DSC-7 instrument. X-ray diffraction patterns were recorded with a Philips APD 3600 instrument using Cu Kα radiation. Optical microscopy was performed using a Leitz microscope equipped with a hot stage. Elemental microanalyses were obtained by Galbraith Laboratories, Knoxville, TN.

Synthesis of $RC_6H_4C_6H_4OH$, Where R = (*S*)-$OCH_2CH(CH_3)CH_2CH_3$ (1). 4,4′-Dihydroxybiphenyl (6.50 g, 34.9 mmol) was dissolved in 95% ethanol (250 mL). Potassium hydroxide (3.94 g, 70.36 mmol) was then added to the solution. The solution was heated to reflux for 15 min to produce the salt. (*S*)-(+)-1-Bromo-2-methylbutane (5.00 g, 33.10 mmol) in 95% ethanol (100 mL) was then added dropwise to the salt solution over 3 h. After the addition was complete, the solution was heated to reflux for 24 h. The solution was allowed to cool to room temperature and was poured into 500 mL of 5% aqueous HCl. The resultant precipitate was collected by vacuum filtration. The white powder was then dissolved in ethyl acetate, and the remaining solids were removed by filtration. The crude product was then purified by column chromatography using 25% ethyl acetate/75% hexane as the eluent to give the product in 30% yield. ^{1}H NMR ($CDCl_3$) δ 1.00 (t, CH_3), 1.05 (d, CH_3), 1.31 (m, CH_2), 1.57 (m, CH_2), 1.88 (m, OCH_2), 6.95 (t, ArH), 7.45 (d, ArH). ^{13}C NMR ($CDCl_3$) δ 11.0, 16.8, 26.1, 29.7, 72.0, 114.5, 128.0, 132.5, 133.6, 157.0, 158.5.

Preparation of $HO(CH_2CH_2O)_mC_6H_4C_6H_4OR$, Where R = (*S*)-$OCH_2CH(CH_3)CH_2CH_3$. The synthesis of compound **3** is described, as the synthesis of compounds **2** and **3** were very similar. To an ethanolic solution of **1** (5.00 g, 19.53 mmol) and potassium hydroxide (1.30 g, 23.21 mmol) was added ((chloroethoxy)ethoxy)ethanol (4.06 g, 24.00 mmol). The solution was heated to reflux for 18 h and was then neutralized with 5% HCl (500 mL). The resultant precipitate was collected by vacuum filtration and was dissolved in chloroform. The chloroform layer was then washed with water (3 × 200 mL) and dried over $MgSO_4$. After removal of the $MgSO_4$ by filtration, the chloroform was removed under reduced pressure with the aid of a rotary evaporator. The crude product was then purified by column chromatography with ethyl acetate as the eluent (yield 50%).

Characterization data for **2**: ^{1}H NMR ($CDCl_3$) δ 1.00 (t, CH_3, 3H), 1.05 (d, CH_3, 3H), 1.31 (m, CH_2, 2H), 1.57 (m, CH_2, 2H), 1.88 (m, OCH_2, 2H), 3.6−4.0 (m, OCH_2, 6H), 4.18 (t, OCH_2, 2H), 6.95 (t, ArH, 4H), 7.45 (d, ArH, 4H). ^{13}C NMR ($CDCl_3$) δ 11.0, 16.8, 26.1, 29.7, 62.2, 67.0, 69.2, 72.0, 72.9, 114.5, 128.0, 132.5, 133.6, 157.0, 158.5. Mp = 116 °C. $[\alpha]^{24} = 9.95°$.

Characterization data for **3**: ^{1}H NMR ($CDCl_3$) δ 0.98 (t, CH_3, 3H), 1.05 (d, CH_3, 3H), 1.30 (m, CH_2, 2H), 1.59 (m, CH_2, 2H), 1.88 (m, OCH_2, 2H), 3.6−4.0 (m, OCH_2, 10H), 4.18 (t, OCH_2, 2H), 6.95 (t, ArH, 4H), 7.45 (d, ArH, 4H). ^{13}C NMR ($CDCl_3$) δ 11.0, 16.8, 26.1, 29.7, 62.2, 67.0, 69.5, 70.5, 71.0, 72.0, 72.5, 114.5, 128.0, 132.5, 133.6, 157.0, 158.5. Mp = 86 °C. $[\alpha]^{24} = 7.19°$.

Typical Single-Substituent Polymer Preparation. Compound **3** (2.53 g, 6.52 mmol) was dissolved in dry THF (50 mL) in a Schlenk flask. This solution was then cannulated into a 100 mL Schlenk flask containing sodium hydride (0.263 g, 6.58 mmol) suspended in 25 mL of THF, and the resultant solution was stirred for 16 h. The sodium salt of **3** was then transferred to an addition funnel and added dropwise over a period of 1 h to a THF solution of poly(dichlorophosphazene) (0.285 g, 2.48 mmol). The solution was then heated to reflux for 6 h. After the solution had cooled to room temperature, it was concentrated using reduced pressure, and the polymer was precipitated into 500 mL of deionized water. The resulting polymer was further purified by reprecipitations from warm THF into H_2O (×2), ethanol (×3), and hexane (×3) (approximate yield, 67%).

Typical Mixed-Substituent Polymer Preparation with Nonmesogenic Cosubstituents. (Methoxyethoxy)ethanol (0.128 g, 1.04 mmol) was added via syringe to NaH (0.025 g, 1.05 mmol) in 60 mL of THF in a Schlenk flask. After the solution had been stirred at room temperature for 2 h, it was cannulated into an addition funnel. The sodium alkoxide was then added dropwise to a solution of poly(dichlorophosphazene) (0.24 g, 2.09 mmol) in 100 mL of THF contained in a 250 mL three-neck round-bottomed flask. The solution was stirred at room temperature for 12 h. Compound **3** (1.12 g, 3.30 mmol) in 20 mL of THF was added via syringe to a Schlenk flask containing NaH (0.078 g, 3.30 mmol) in 50 mL of THF and stirred for 2 h. The salt was then cannulated into an addition funnel and added dropwise to the polymer solution. After the solution had been stirred for 24 h at room temperature, it was concentrated using a rotary evaporator. The polymer was then purified by reprecipitations into H_2O (×2), ethanol (×3), and hexanes (×3) (approximate yield, 80%).

Typical Mixed-Substituent Polymer Preparation with Mesogenic Cosubstituents. Compound **3** (1.25 g, 3.63 mmol) was dissolved in 10 mL of THF and syringed into a Schlenk flask which contained NaH (0.091 g, 3.73 mmol) in 50 mL of THF. The solution was stirred at room temperature for 2 h and was then cannulated into an addition funnel. The alkoxide was then added to poly(dichlorophosphazene) (0.26 g, 2.26 mmol) in 150 mL of THF, and the solution was stirred for 12 h at room temperature. Compound **4** (0.88 g, 2.27 mmol) was dissolved in 10 mL of THF syringed into a Schlenk flask containing NaH (0.060 g, 2.50 mmol) in 50 mL of THF. The

solution was stirred for 2 h and then cannulated into an addition funnel. The alkoxide was then added dropwise to the polymer solution, and the solution was stirred at room temperature for 20 h. The polymer solution was concentrated on a rotary evaporator and purified by reprecipitations into H_2O (×2), ethanol (×3), and hexanes (×3) (approximate yield, 70%).

Film Preparation for X-ray Diffraction and Optical Hot Stage Microscopy. The polymers were cast onto glass slides from either THF or $CHCl_3$ solutions. All the films were ca. 10 μm thick by scanning electron microscopy analysis. X-ray diffraction samples were made by quenching these films from the appropriate temperature. To do this, the films were removed from the hot stage at the desired temperature and quickly placed onto a metal plate which was cooled to 0 °C.

Acknowledgment. The authors thank the Office of Naval Research and Corning Inc. for their support of this work. X-ray analyses were performed at the Intercollege Materials Research Lab at The Pennsylvania State University. Transmission electron microscopy and scanning electron microscopy experiments were carried out at the Electron Microscope Facility for the Life Sciences in the Biotechnology Institute at The Pennsylvania State University. The authors also thank Else Breval for the many useful discussions concerning optical microscopy and for the use of her equipment to obtain the optical micrographs.

References and Notes

(1) Ciferri, A.; Krigbaum, W. R.; Mayer, R. B. *Polymer Liquid Crystals*; Academic Press: New York, 1982; pp 248–273.
(2) *Phys. Today* **1982**, *35*, 5.
(3) Blumstein, A. *Polymeric Liquid Crystals*; Academic Press: New York, 1985.
(4) Plate, N. A.; Shibaev, V. P. *Comb-Shaped Polymers and Liquid Crystals*; Plenum Press: New York, 1987; pp 376–378.
(5) Decobert, G.; Dubois, J. C.; Esselin, S.; Noel, C. *Liq. Cryst.* **1986**, *1*, (4), 307.
(6) Bernev, L. A.; Blinov, L. M.; Osipov, M. A.; Pikin, S. A. *Mol. Cryst. Liq. Cryst.* **1988**, *158A*, 3.
(7) Goodby, J. W.; Lesilie, T. M. *Mol. Cryst. Liq. Cryst.* **1984**, *110*, 175.
(8) Lipatov, Y. S.; Tsukruk, V. V.; Shilov, V. V. *Rev. Macromol. Chem. Phys.* **1984**, *24* (2), 173.
(9) Godovsky, Yu. K.; Papkov, V. S. *Adv. Polym. Sci.* **1989**, *88*.
(10) Wunderlich, B.; Grebowicz, J. *Adv. Polym. Sci.* **1984**, *60/61*.
(11) Allcock, H. R.; Kugel, R. L. *J. Am. Chem. Soc.* **1965**, *87*, 4216.
(12) Allcock, H. R. *Chem. Eng. News* **1985**, *63*, 22.
(13) Allcock, H. R. *Phosphorus–Nitrogen Compounds (Cyclic, Linear, and High Polymeric Systems)*; Academic Press: New York, 1972.
(14) Allcock, H. R.; Connolly, M. S.; Suszko, J. T.; Al-Shali, S. *Macromolecules* **1988**, *21*, 323.
(15) Allcock, H. R.; Allen, R. W.; Meister, J. J. *Macromolecules* **1976**, *9*, 950.
(16) Allcock, H. R.; Arcus, R. A. *Macromolecules* **1979**, *12*, 1130.
(17) Allcock, H. R.; Arcus, R. A. *Macromolecules* **1980**, *13*, 919.
(18) Allcock, H. R.; Kugel, R. L.; Valan, K. J. *Inorg. Chem.* **1966**, *5*, 1709.
(19) Allcock, H. R.; Kugel, R. L. *Inorg. Chem.* **1963**, *2*, 896.
(20) Paciorek, K. L. *Inorg. Chem.* **1964**, *3*, 96.
(21) Allcock, H. R. *J. Am. Chem. Soc.* **1964**, *86*, 2591.
(22) Allcock, H. R.; Kugel, R. L. *Inorg. Chem.* **1966**, *5*, 1016.
(23) Allen, G. J.; Lewis, J.; Todd, S. M. *Polymer* **1970**, *11*, 14.
(24) Singler, R. E.; Schneider, N. S.; Hagnauer, G. L. *Polym. Eng. Sci.* **1975**, *15*, 321.
(25) Kojma, M.; Magill, J. H. *Makromol. Chem.* **1985**, *189*, 649.
(26) Wunderlich, B.; Grebowicz, J. *Adv. Polym. Sci.* **1984**, *60/61*, 1.
(27) Ferrar, W. T.; Marshall, A. S.; Whitefield, J. *Macromolecules* **1987**, *20*, 317.
(28) Allcock, H. R.; Kim, C. *Macromolecules* **1991**, *24*, 2841.
(29) Allcock, H. R.; Kim, C. *Macromolecules* **1990**, *23*, 3881.
(30) Allcock, H. R.; Kim, C. *Macromolecules* **1989**, *22*, 2596.
(31) Allcock, H. R.; Kim, C. *Macromolecules* **1987**, *20*, 1726.
(32) Percec, V.; Tomazos, D.; Willingham, R. A. *Polym. Bull.* **1989**, *22*, 199.
(33) Singler, R. E.; Willingham, R. A.; Noel, C.; Friedrich, C.; Bosio, L.; Atkins, E. D. T. *Macromolecules* **1991**, *24*, 510.
(34) Singler, R. E.; Jaglowski, A. J.; Sullivan, A. D.; Willingham, R. A. *Polym. Prepr. (Am. Chem. Soc., Div. Polym. Chem.)* **1990**, *31* (1), 488.
(35) Singler, R. E.; Willingham, R. A.; Noel, C.; Friedrich, C.; Bosio, L.; Atkins, E. D. T.; Lenz, R. W. *Polym. Prepr. (Am. Chem. Soc., Div. Polym. Chem.)* **1989**, *30* (2), 491.
(36) Singler, R. E.; Willingham, R. A.; Lenz, R. W.; Furukawa, A.; Finkelman, H. *Macromolecules* **1987**, *20*, 1727.
(37) Japanese Patent 04257594, 1992 (CA119(10):106360h).
(38) Meyer, R. B.; Liebert, L.; Strzeleck, L.; Keller, P. *J. Phys. Chem.* **1975**, 36.
(39) Clark, N. A.; Lagerwall, S. T. *Appl. Phys. Lett.* **1980**, *36* (11), 899.
(40) Yu, L. J.; Lee, H.; Bak, C. S.; Labes, M. M. *Phys. Rev. Lett.* **1976**, *36* (7), 388.
(41) Shibaev, V. P.; Kozlovsky, M. V.; Berenev, L. A.; Blinov, L. M.; Plate, N. A. *Polym. Bull.* **1984**, *12*, 299.
(42) Schiekel, M. F.; Fahrenschen, K. *Appl. Phys. Lett.* **1971**, *19* (10), 391.
(43) Soref, R. A.; Rafus, M. J. *J. Appl. Phys.* **1972**, *43* (5), 2029.
(44) Kahn, F. J. *Appl. Phys. Lett.* **1972**, *30* (5), 199.
(45) Chiellini, E.; Galli, G.; Cioni, F.; Dossi, E. *Makromol. Chem., Macromol Symp.* **1993**, *69*, 51.
(46) Weiss, R. A.; Ober, C. K. *Liquid-Crystalline Polymers*; ACS Symposium Series 435; American Chemical Society: Washington, DC, 1990; Chapter 14.
(47) Heavin, S. D.; Fung, B. M.; Sluss, J. J., Jr.; Batchman, T. E. *Mol. Cryst. Liq. Cryst.* **1994**, *238*, 83.
(48) Molecular moldeling program used was Quanta 3.0. Molecular lengths were measured after using the CHARMm minimization program. The software is licensed by Polygen Corp. (copyright 1990).
(49) McArdle, C. B., Ed. *Side Chain Liquid Crystalline Polymers*; Chapman and Hall: New York, 1989.
(50) Engel, M.; Hisgen, E.; Keller, R.; Kreuder, W.; Reck, B.; Ringsdorf, H.; Schadt, H.-W.; Tschirner, P. *Pure Appl. Chem.* **1985**, *57*, 109.
(51) Shibaev, V.; Plate, N. *Adv. Polym. Sci.* **1984**, *60/61*, 173.

MA946522E